CONEM 2010
VI Congresso Nacional de Engenharia Mecânica

ABCM
ASSOCIAÇÃO BRASILEIRA DE ENGENHARIA E CIÊNCIAS MECÂNICAS
COMPROMETIDA COM A PROMOÇÃO DO DESENVOLVIMENTO DA ENGENHARIA E DAS CIÊNCIAS MECÂNICAS

VI CONGRESSO NACIONAL DE ENGENHARIA MECÂNICA
VI NATIONAL CONGRESS OF MECHANICAL ENGINEERING
18 a 21 de agosto de 2010 – Campina Grande – Paraíba - Brasil
August 18 – 21, 2010 – Campina Grande – Paraíba – Brazil

A NEW POLYNOMIAL UPWIND CONVECTION SCHEME FOR FLUID FLOW SIMULATIONS

Laís Corrêa, lacorrea@icmc.usp.br[1]
Giseli Aparecida Braz de Lima, giabl@icmc.usp.br[1]
Patricia Sartori, psartori@icmc.usp.br[1]
Miguel Antonio Caro Candezano, mcaro@icmc.usp.br[1]
Valdemir Garcia Ferreira, pvgf@icmc.usp.br[1]

[1]Instituto de Ciências Matemáticas e de Computação - USP, Av. Trabalhador São-carlense, 400 - CEP: 13560-970 - São Carlos - SP.

Abstract. *The simulation of fluid flow problems involving strong convective character is a difficult problem to be solved and has attracted many researchers in the CFD community. In this scenario, we present in this work a new polynomial upwind scheme, called SDPUS-C1, for numerical solution of conservation laws and related fluid dynamics problems. The scheme is developed in the context of normalized variables (NV) of Leonard and satisfies the CBC and TVD stability criteria of Gaskell and Lau, and Harten, respectively. The scheme was implemented into the CLAWPACK and Freeflow codes. The numerical solutions obtained with this scheme can achieve second/third order of accuracy in smooth regions and first order near to discontinuities (shocks). The performance of the SDPUS-C1 is assessed in the solution of linear and nonlinear hyperbolic systems, such as shallow water, acoustics, and Euler equations. As application, the scheme is then used in the solution of incompressible Navier-Stokes equations in cylindrical coordinate system. From numerical results, one can clearly see that the SDPUS-C1 scheme is a robust tool for resolving both compressible and incompressible complex flow problems.*

Keywords: *convective schemes, conservation laws, Navier-Stokes equations*

1. INTRODUCTION

Many numerical difficulties are encountered when one intends to approximate the convection terms (in general nonlinear) in hyperbolic conservation laws and related fluid dynamics problems. Because of this, the search for a new high resolution upwinding scheme for modeling these terms has attracted many researchers in CFD community; and several attempts have been made in this direction. The major obstacle has been to develop a scheme that captures discontinuities (or shock waves), commonly encountered in fluid flow simulations. In addition, one seeks such a scheme that achieves high accuracy (in general ≥ 2), stability, preservation of monotonicity, economy and simplicity of implementation. This is the prime motivation for the development of the new upwinding scheme presented here.

The objective of this work is to present a new polynomial upwind scheme, called SDPUS-C1 (*Six-Degree Polynomial Upwind Scheme of C^1 Class*), for numerical solution of hyperbolic conservation laws and compressible/incompressible fluid flow equations. The performance of the scheme is assessed in resolving conservation laws formulated by linear and nonlinear hyperbolic systems, namely 1D/2D shallow water, 2D acoustics and 2D Euler equations. For lack of space, we compare the numerical solutions with reference solutions using fine meshes. As an application, the new scheme is then used for solving 2D Navier-Stokes equations in cylindrical coordinate system (2D-1/2).

2. NORMALIZED VARIABLES AND CBC/TVD STABILITY CRITERIA

The SDPUS-C1 scheme is used to interpolate a numerical flux, say ϕ_f, at the face f using three neighboring mesh points, namely D (*Downstream*), U (*Upstream*) and R (*Remote-upstream*), and the convecting velocity V_f at this face. Figure (1) depicts, in 1D case, two situations that occur in our implementation. In the multidimensional case, this upwind-biased strategy is handled in the same fashion.

By using the well known upwinding strategy (see, for example, Ferreira (2009)), a scheme is written in the following form (in general nonlinear):

$$\phi_f = \phi_f(D, U, R). \tag{1}$$

In order to simplify the functional relationship given by Eq. (1), linking ϕ_D, ϕ_U and ϕ_R, the original variables are

Figure 1. **Position of compute nodes D, U and R according to the sign of V_f speed of a convective variable ϕ_f.**

transformed in NV of Leonard (1988) as

$$\hat{\phi_{()}} = \frac{\phi_{()} - \phi_R}{\phi_D - \phi_R}. \tag{2}$$

According to Leonard (1988), the functional relationship in Eq. (2) is the basis for constructing an upwinding scheme in NV. In this sense, it is possible to derive a nonlinear monotonic third-order NV scheme by imposing the following conditions, for $0 \leq \hat{\phi}_U \leq 1$: $\hat{\phi}_f(0) = 0$ (a necessary condition), $\hat{\phi}_f(1) = 1$ (a necessary condition), $\hat{\phi}_f(0.5) = 0.75$ (a necessary and sufficient condition to reach second order of accuracy) and $\hat{\phi}'_f(0.5) = 0.75$ (a necessary and sufficient condition to reach third order of accuracy). Leonard (1988) also recommends that for values of $\hat{\phi}_U < 0$ or $\hat{\phi}_U > 1$, the scheme must be extended in a continuous manner using the FOU (*First Order Upwinding*) scheme which is defined by $\hat{\phi}_f = \hat{\phi}_U$. Gaskell and Lau (1988) provide the convection-boundedness criterion (CBC), which states the conditions for boundedness:

$$- \ \hat{\phi}_U \leq \hat{\phi}_f(\hat{\phi}_U) \leq 1, \qquad \text{if } \hat{\phi}_U \in [0,1];$$

$$- \ \hat{\phi}_f = \hat{\phi}_f(\hat{\phi}_U) = \hat{\phi}_U, \qquad \text{if } \hat{\phi}_U \notin [0,1]; \tag{3}$$

$$- \ \hat{\phi}_f(0) = 0 \text{ and } \hat{\phi}_f(1) = 1.$$

The CBC has long been accepted as both sufficient and necessary condition for a scheme possessing boundedness (see Gaskell and Lau (1988)). It can also be shown that the CBC can guarantee the stability of a scheme (see Yu *et al.* (2001)).

Another important convective stability is the total-variation diminishing (TVD) constraint of Harten (1983), a purely scalar property. This property ensures that spurious oscillations (unphysical noises) are removed from the numerical solution of a conservation law. Formally, consider a sequence of discrete approximations $\phi(t) = \phi_i(t)_{i\in\mathbf{Z}}$ for a scalar quantity. The total-variation (TV) at time t of this sequence is defined by

$$TV(\phi(t)) = \sum_{i\in\mathbf{Z}} |\phi_{i+1}(t) - \phi_i(t)|. \tag{4}$$

From this, by definition, we say that the scheme is TVD if, for all data set ϕ^n, the values ϕ^{n+1} calculated by numerical method satisfy

$$TV(\phi^{n+1}) \leq TV(\phi^n), \quad \forall n. \tag{5}$$

It is important to emphasize, from numerical point of view, that TVD schemes are very attractive: guarantee convergence, monotonicity and high order accuracy.

3. DEVELOPMENT OF THE SDPUS-C1 SCHEME

In this section, we present the derivation of the SDPUS-C1 scheme by assuming that the NV at the cell interface f, $\hat{\phi}_f$, are related to $\hat{\phi}_U$ as part of a six-degree polynomial function

$$\hat{\phi}_f = \sum_{k=0}^{6} a_k \hat{\phi}_U^k, \tag{6}$$

for $0 \leq \hat{\phi}_U \leq 1$, and the FOU scheme for $\hat{\phi}_U < 0$ or $\hat{\phi}_U > 1$. By considering the coefficient a_2 as a free parameter, say γ, the other coefficients in Eq. (6) are determined by imposing the four conditions of Leonard (1988) presented above plus the condition that this polynomial function is continuously differentiable. For this, the function is linked at the points $(0,0)$ and $(1,1)$ with the same values of the first derivatives. Thus, the SDUPS-C1 scheme is a continuously differentiable function across domain. And, according to Lin and Chieng (1991), it is important to note that this property avoids convergence problems when coarse meshes are employed.

In summary, the convection upwind SDUPS-C1 scheme is given by

$$\hat{\phi}_f = \begin{cases} (-24+4\gamma)\hat{\phi}_U^6+(68-12\gamma)\hat{\phi}_U^5+(-64+13\gamma)\hat{\phi}_U^4+(20-6\gamma)\hat{\phi}_U^3+\gamma\hat{\phi}_U^2+\hat{\phi}_U, & \text{if} \quad \hat{\phi}_U \in [0,1], \\ \hat{\phi}_U, & \text{if} \quad \hat{\phi}_U \notin [0,1]. \end{cases} \tag{7}$$

The corresponding flux limiter function for the SDPUS-C1 scheme is derived as follow. The Eq. (7) (see Waterson and Deconinck (2007)) can be write as

$$\hat{\phi}_f = \hat{\phi}_U + \frac{1}{2}\psi(r_f)(1-\hat{\phi}_U), \tag{8}$$

where $\psi(r_f) = \psi_f$ is the flux limiter function and r_f is the reason of two consecutive gradients (a sensor). In NV this reason is given by

$$r_f = \frac{1}{1-\hat{\phi}_U}. \tag{9}$$

By combining Eqs. (7), (8) and (9), we deduce the flux limiter function for the SDPUS-C1 scheme, namely

$$\psi(r_f) = \begin{cases} \dfrac{(-8+2\gamma){r_f}^4+(40-4\gamma){r_f}^3+2\gamma {r_f}^2}{(1+r_f)^5}, & \text{if} \quad r_f \geq 0, \\ 0, & \text{if} \quad r_f < 0. \end{cases} \tag{10}$$

In a more widely used notation (see, e.g., Waterson and Deconinck (2007)), the flux limiter Eq. (10) can also be written as

$$\psi(r_f) = \max\left\{0, \ \frac{0.5(|r_f|+r_f)[(-8+2\gamma)r_f^3+(40-4\gamma)r_f^2+2\gamma r_f]}{(1+|r_f|)^5}\right\}. \tag{11}$$

It is important to observe that the SDPUS-C1 scheme is TVD $\forall\gamma \in [4,12]$ (see Fig. (2)-(a)) and, consequently, into the CBC region. The SDPUS-C1 flux limiter function is depicted in Fig. (2)-(b). In this work, we used $\gamma = 12$ in all computation since this value has provided the best results in all tests.

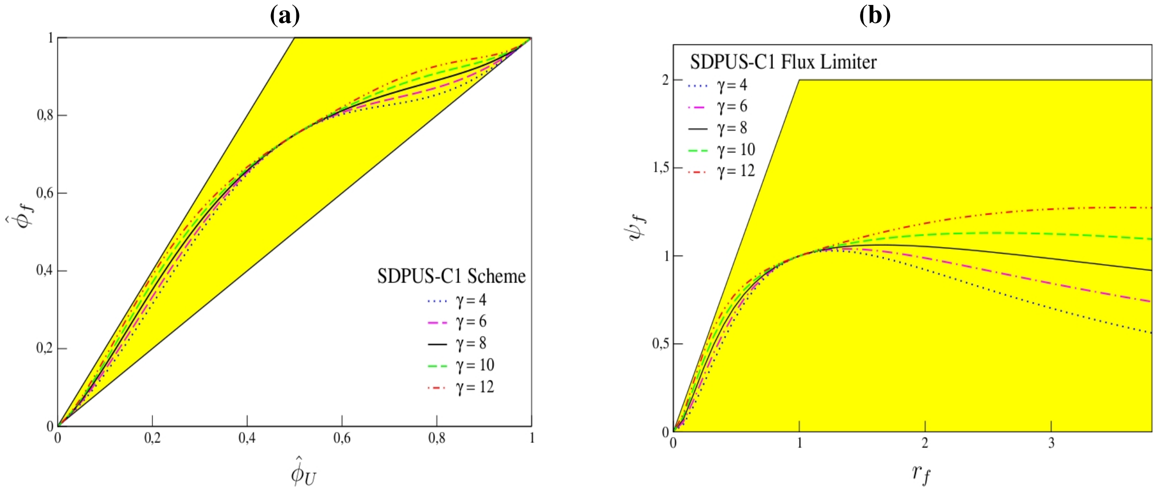

Figure 2. **SDPUS-C1 scheme in (a) normalized variables and (b) this flux limiter in TVD region.**

Note that the SDPUS-C1 scheme is monotone and second order accuracy, since its limiter Eq. (10), for $r \geq 0$, $\forall\gamma$, satisfies the condition introduced by Waterson and Deconinck (2007), namely a scheme must respect the linear variation of the solution, satisfying $\psi(1) = 1$, which is also a necessary condition for achieving second order accuracy on uniform meshes. In addition, the SDPUS-C1 scheme can achieve third order accuracy, since its limiter Eq. (10), for $r \geq 0$, $\forall\gamma$, satisfies $\psi^{'}(1) = \frac{1}{4}$ (see Zijlema (1996)), which is a necessary and sufficient condition to achieve third order accuracy.

4. NUMERICAL RESULTS

In order to demonstrate the behavior, validity, flexibility and robustness of the SDPUS-C1 scheme, in this section we solve various linear and nonlinear problems such as 1D/2D shallow water, 2D acoustics and 2D Euler equations. For this, we have used the well recognized CLAWPACK (Conservation LAW PACKage) software of LeVeque *et al.* (2002) equipped with the SDPUS-C1 scheme. And as an application, the SDPUS-C1 scheme is applied for solving 2D incompressible Navier-Stokes equations in cylindrical coordinate system using the current Freeflow code of Castelo *et al.* (2000).

4.1 1D Conservation Laws

Many problems in fluid dynamics that involve conservation of quantities are modeled by hyperbolic conservation laws. In particular, in the 1D case these equations are given by

$$\phi_t + F(\phi)_x = 0, \tag{12}$$

where $\phi = \phi(x,t)$ represents the conserved variable vector and $F(\phi) = F(\phi(x,t))$ is the flux function vector.

4.1.1 Shallow Water Equations

These equations model the dynamics of an incompressible fluid involving a free surface in a tube with horizontal velocity $\phi(x,t)$ (the vertical velocity is neglected). The nonlinear hyperbolic system of shallow water is given by Eq. (12) with $\phi = [h, hu]^T$ e $F(\phi) = [hu, hu^2 + \frac{1}{2}gh^2]^T$, where h is the height of the fluid (in this case water), hu is the discharge and g the acceleration due to gravity. In this work, we applied the shallow water system to solve the dam-break problem, which models a dam that breaks at $t = 0$. This Riemann problem is formed by the system Eq. (12), with the conserved variables and flux vectors given above, defined for $x \in [-5, 5]$ and with the initial conditions

$$u_0(x) = 0 \quad \text{and} \quad h_0(x) = \begin{cases} 3, & \text{if} \quad x \leq 0, \\ 1, & \text{if} \quad x > 0. \end{cases} \tag{13}$$

In this simulation, we used a mesh size of $N = 200$ computational cells, the Courant number $\theta = 0.8$ and the final simulation time $t = 2.0$. As a reference solution, we considered the numerical solution obtained with the Godunov scheme of the first order (see LeVeque (2002)) using a mesh size of $N = 10000$ computational cells. The numerical results are presented in Fig. (3). As one can see from this figure, the results with the SDPUS-C1 scheme are, in general, in good agreement with the reference solution. From this same figure, it can be seen discrepancies near to $x = -3.5$ and $x = 3$. These differences can be attributed to the size of the mesh.

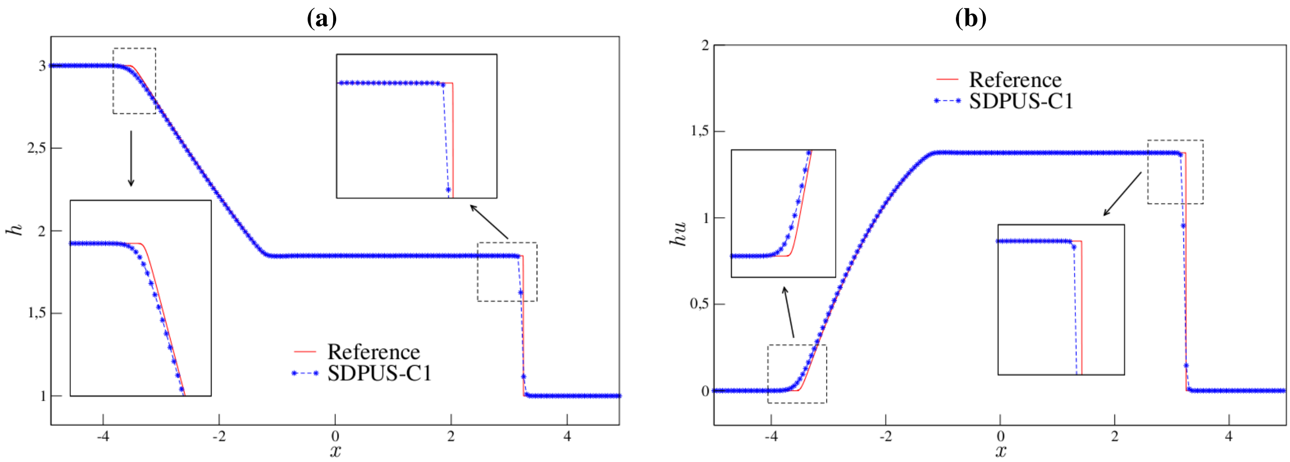

Figure 3. **Reference and numerical solutions for: (a) depth h and (b) discharge hu for the dam-break problem.**

4.2 2D Conservation Laws

For the 2D case, the conservations laws are given by

$$\phi_t + F(\phi)_x + G(\phi)_y = 0, \tag{14}$$

where $\phi = \phi(x,y,t)$ is the conserved variable vector, and $F(\phi) = F(\phi(x,y,t))$ and $G(\phi) = G(\phi(x,y,t))$ are the flux functions vector.

4.2.1 Acoustics Equations

In this section, we solve the 2D linear hyperbolic system for acoustics in a heterogeneous (piecewise constant) medium with variable coefficients which is given by Eq. (14). In this system $\phi = [p, u, v]^T$, $F(\phi) = [Ku, p/\rho, 0]^T$ and $G(\phi) = [Kv, 0, p/\rho]^T$, being $[u, v]^T$ the velocity vector, and K, ρ and p, bulk modulus of compressibility of the material, density and pressure, respectively (for details, the reader is referred to LeVeque (2002)). This system is solved in the domain $\Omega = [0,1] \times [0,1]$, where the interface $x = 0.5$ separates two materials (one on the left and another on the right) with density

ρ and sound speed c given by $\rho_L = 1$, $c_L = 1$, and $\rho_R = 4$, $c_R = 0.5$. Another datum for the simulation is a pulse for the pressure which leads to a radially-symmetric pressure disturbance, namely

$$r = \sqrt{(x - 0.25)^2 + (y - 0.4)^2}. \tag{15}$$

The initial conditions are

$$p_0 = \begin{cases} 1 + 0.5\left[\cos\left(\frac{\pi \cdot r}{0.1}\right) - 1\right], \text{ if} & r < 0.1, \\ 0, & \text{otherwise,} \end{cases} \qquad u_0 = 0, \qquad v_0 = 0. \tag{16}$$

For the simulation of this problem, we consider the Godunov method with a correction term contemplating the SDPUS-C1 (or the MC (*monotonized central-difference*) for obtaining the reference solution) as the flux limiter. The numerical solution using the SDPUS-C1 was obtained in a mesh size of 200×200 computational cells and Courant number $\theta = 0.8$, while the reference solution was calculated in a mesh size of 400×400 computational cells and Courant number $\theta = 0.8$. Figure (4) shows the cross-section from the simulation of the pressure at $t = 0.4$. One can observe from this figure that when the pressure pulse hits the interface, it is partially reflected and partially transmitted. From the same figure, the SDPUS-C1 scheme provides results in good agreement with reference solutions. In order to complete the analysis, we calculated the pressure variation as a function of distance from the origin (ie, p in $y = 0$), as shown in Fig. (5), which compares the SDPUS-C1 scheme with the reference solution, showing that the new scheme has good performance.

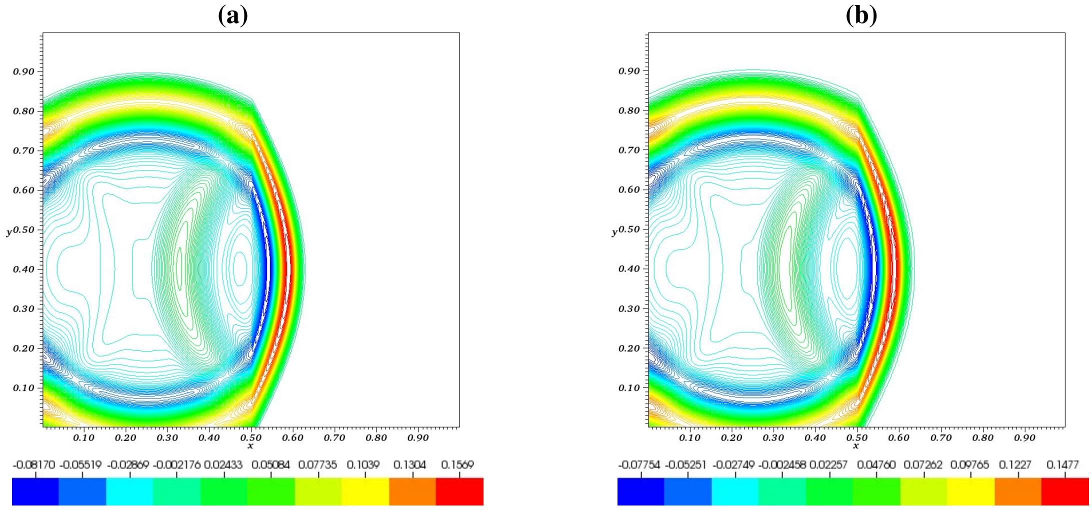

Figure 4. **(a) Reference and (b) numerical solutions for the boundary pressure p.**

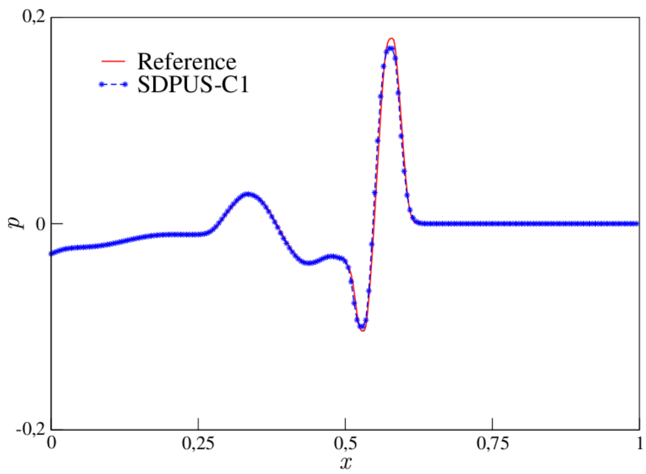

Figure 5. **Comparison of the reference and numerical solutions for the pressure p in $y = 0$.**

4.2.2 Shallow Water Equations

The 2D nonlinear hyperbolic shallow water equations are given by Eq. (14) with $\phi = [h, hu, hv]^T$, $F(\phi) = [hu, hu^2 + \frac{1}{2}gh^2, huv]^T$ and $G(\phi) = [hu, huv, hv^2 + \frac{1}{2}gh^2]^T$, in which h represents the height of the fluid, $[u, v]^T$

and $[hu, hv]^T$ are, respectively, the velocity and discharge vectors, and g is the acceleration due to gravity. In order to verify the performance of the SDPUS-C1 scheme for solving this hyperbolic system, we simulated a radial dam-break problem (see, for instance, LeVeque *et al.* (2002)). In summary, the problem models a dam, initially at rest, dividing the domain $\Omega = [-2.5, 2.5] \times [-2.5, 2.5]$ in two parts (inside of the dam and outside of it). At $t = 0$, the dam is removed forming a shock wave, that travels radially outwards while a rarefaction wave propagates inwards. This problem is illustrated in Fig. (6) (case (a) at $t = 0$ and case (b) at $t = 0.25$), where the depth is initially $h = 2$ inside a dam and $h = 1$ outside.

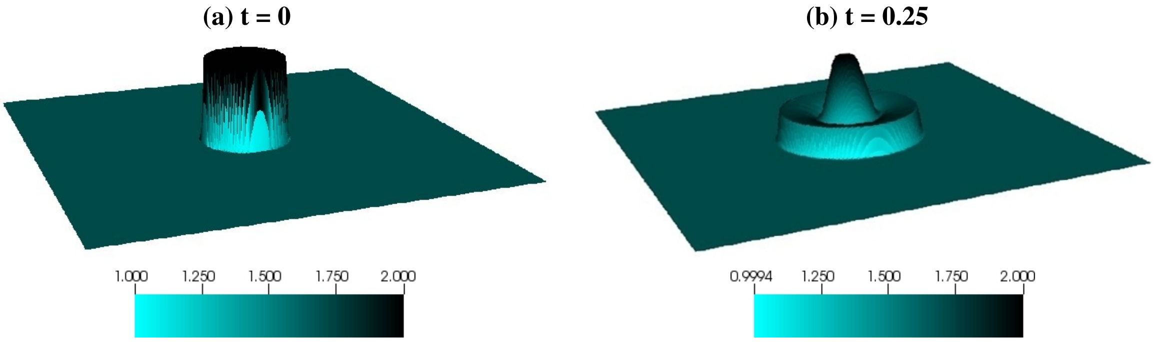

Figure 6. **The radial dam-break problem (a) in $t = 0$ and (b) $t = 0.25$.**

For the simulation of this problem, we consider the Godunov method with a correction term contemplating the SDPUS-C1 (or the MC (*monotonized central-difference*) for obtaining the reference solution) as the flux limiter. The numerical solution using the SDPUS-C1 was obtained in a mesh size of 125×125 computational cells and Courant number $\theta = 0.8$, while the reference solution was calculated in a mesh size of 250×250 computational cells and Courant number $\theta = 0.5$. The results of this simulation for h profile (cross section), at the $x \perp y$ plane and final time $t = 1.5$, are shown in Fig. (7), where case (a) of this figure corresponds to the reference solution and case (b) to the numerical solution with SDPUS-C1. By analyzing this figure, we can observe that the results obtained with the SDPUS-C1 scheme are satisfactorily consistent with those of the reference solution. In order to complete the analysis, we calculated the depth variation as a function of distance from the origin (ie, h in $y = 0$), as shown in Fig. (8), which compares the SDPUS-C1 scheme with the reference solution, showing that the new scheme has good performance.

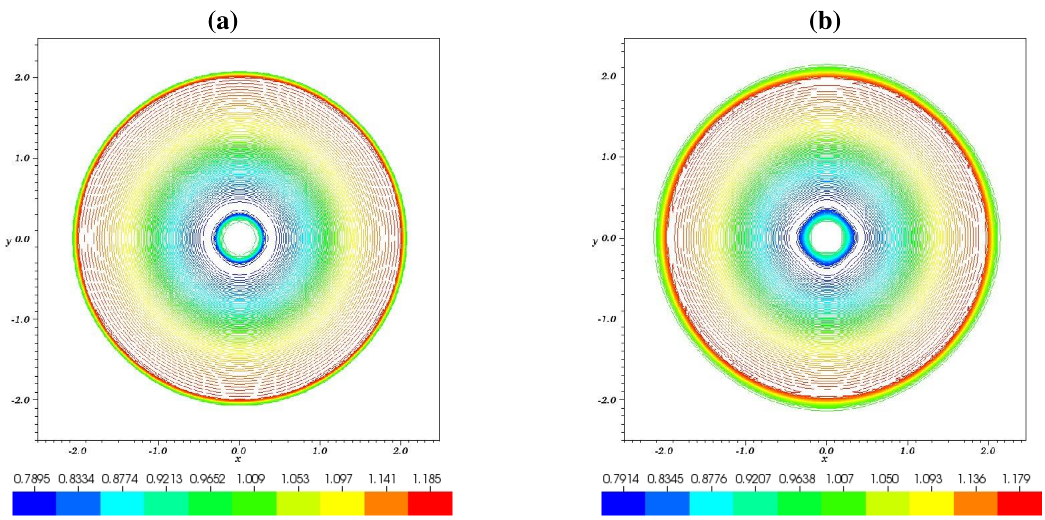

Figure 7. h **profiles for the radial dam-break problem: (a) reference and (b) numerical solutions with SDPUS-C1.**

4.2.3 Euler Equations of Gas Dynamics

The 2D Euler equations of gas dynamics are given by Eq. (14), where $\phi = [\rho, \rho u, \rho v, E]^T$, $F(\phi) = [\rho u, \rho u^2 + p, \rho uv, (E + p)u]^T$ and $G(\phi) = [\rho v, \rho uv, \rho v^2 + p, (E + p)v]^T$, being $[\rho u, \rho v]^T$ the momentum vector and E is the total energy. To close the system formed by ϕ, $F(\phi)$ and $G(\phi)$, it was considered the ideal gas equation

$$p = (\lambda - 1)(E - \frac{1}{2}\rho(u^2 + v^2)), \tag{17}$$

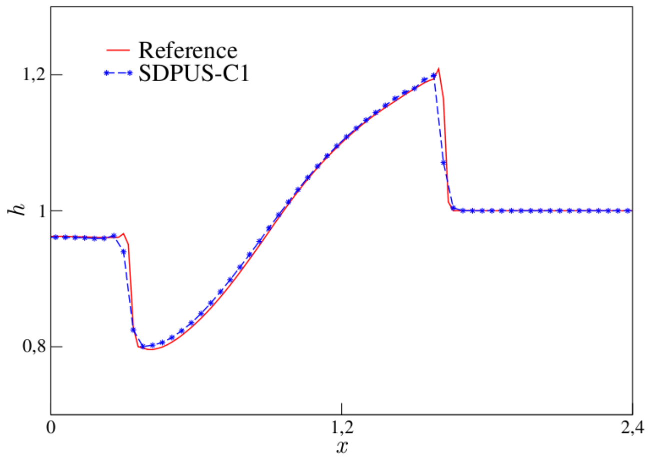

Figure 8. **Comparison of the reference and numerical solutions for the depth h in $y = 0$.**

where $\lambda = 1.4$ is the reason of specific heat. The problem to be simulated here is the *shock-shock interaction* described by Ricchiuto (2005), which consists in the interation of two oblique shocks (states a and c) with two normal shocks (states b and d). The considered domain is $\Omega = [0,1] \times [0,1]$ and the Euler equations are supplemented with the initial conditions

$$[\rho_0,\ u_0,\ v_0,\ p_0]^T = \begin{cases} [1.5,\ 0,\ 0,\ 1.5]^T, & \text{state a,} \\ [0.13799,\ 1.2060454,\ 1.2060454,\ 0.0290323]^T, & \text{state b,} \\ [0.5322581,\ 1.2060454,\ 0,\ 0.3]^T, & \text{state c,} \\ [0.5322581,\ 0,\ 1.2060454,\ 0.3]^T, & \text{state d.} \end{cases} \tag{18}$$

For the simulation, we consider the Godunov method with a correction term contemplating the SDPUS-C1 (or the MC (*monotonized central-difference*) for obtaining the reference solution) as the flux limiter. The numerical solution using the SDPUS-C1 was obtained in a mesh size of 125×125 computational cells and Courant number $\theta = 0.8$, while the reference solution was calculated in a mesh size of 250×250 computational cells and Courant number $\theta = 0.5$. Figure (9) shows the results for contours of the density ρ at time $t = 0.8$. It can be seen, from these figures, that the SDPUS-C1 scheme works very well and provides results in good agreement with the reference solution. In order to complete the analysis, we calculated the density variation as a function of distance from the origin (ie, ρ in $y = 0$), as shown in Fig. (10), which compares the SDPUS-C1 scheme with the reference solution, showing that the new scheme has good performance.

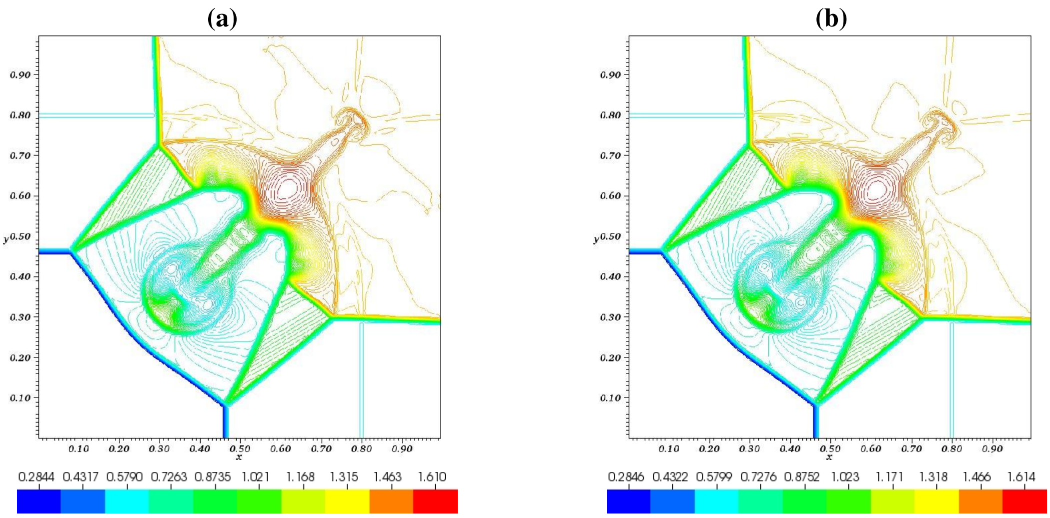

Figure 9. *Shock-shock interaction* **problem, showing the density contours: (a) reference and (b) numerical solutions.**

4.3 Axisymmetric Navier-Stokes Equations

These equations model incompressible fluid flow problems both in laminar and turbulent regimes. In the case of the fluid to be considered a homogeneous medium, the density of the particles does not vary during the movement and the transport properties are constant, the mathematical equations of physical conservation laws for simulation of laminar

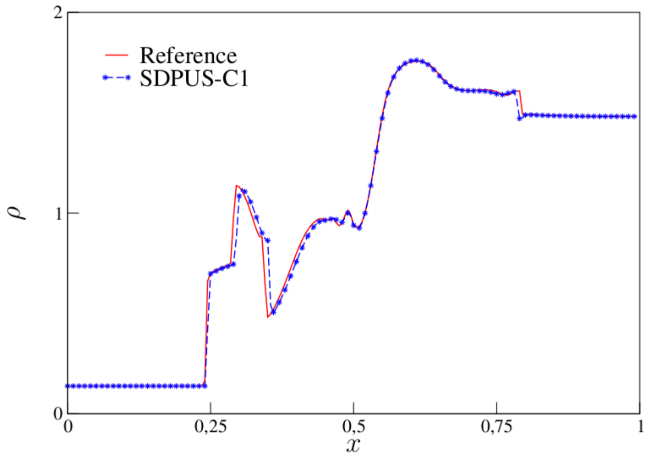

Figure 10. **Comparison of the reference and numerical solutions for the density ρ in $y = 0$.**

flows are the instantaneous Navier-Stokes and continuity equations, which in cylindrical coordinates system (2D-1/2) are given by

$$\frac{\partial u}{\partial t} + \frac{1}{r}\frac{\partial (ruu)}{\partial r} + \frac{\partial (uv)}{\partial z} = -\frac{\partial p}{\partial r} + \frac{1}{Re}\frac{\partial}{\partial z}\left(\frac{\partial u}{\partial z} - \frac{\partial v}{\partial r}\right) + \frac{1}{Fr^2}g_r, \quad (19)$$

$$\frac{\partial v}{\partial t} + \frac{1}{r}\frac{\partial (rvu)}{\partial r} + \frac{\partial (vv)}{\partial z} = -\frac{\partial p}{\partial z} + \frac{1}{Re}\frac{1}{r}\frac{\partial}{\partial r}\left(r\frac{\partial u}{\partial z} - \frac{\partial v}{\partial r}\right) + \frac{1}{Fr^2}g_z, \quad (20)$$

$$\frac{1}{r}\frac{\partial (ru)}{\partial r} + \frac{\partial v}{\partial z} = 0, \quad (21)$$

where t is time, $u = u(r, z, t)$ and $v = v(r, z, t)$ are, respectively, the components of velocity vector in the r and z directions, $g = (g_r, g_z)^T$ is the acceleration due to gravity, with $g_r = 0m/s^2$ and $g_z = 9.81m/s^2$, and p is the pressure (more specifically, pressure divided by density). The dimensionless parameters $Re = U_0 L_0/\nu$ and $Fr = U_0/\sqrt{L_0 g}$ represent, respectively, the Reynolds and Froud numbers, ν being the coefficient of kinematic viscosity given by $\nu = \frac{\mu}{\rho}$, where μ is the dynamic viscosity. Finally, U_0 and L_0 are characteristic scales for velocity and length, respectively.

Equations (19), (20) and (21) were applied for solving the problem of a vertical free jet penetrating into a recipient with the same fluid at rest. The experiment was realized by Taylor (1974), and we used this problem to validate our numerical method (Freeflow) equipped with the SDPUS-C1 scheme. For the simulation of this incompressible flow involving free surfaces, we consider a cylindrical container with $0.06m$ of radius and $0.17m$ in height; the fluid inside container possesses $0.16m$ of height and the injector, with $0.03m$ in height and $0.002m$ of radius, is positioned at $0.1m$ from the free surface of the fluid at rest. The scales involved are $U_0 = 0.5m/s$ and $L_0 = 0.004m$. The dimensionless Reynolds and Froude numbers are $Re = 200$ and $Fr = 2.52409$. Figure (11) shows both (a) experimental and (b) numerical results in times $t = 0.25s$ and $t = 0.75s$. From this figure, one can clearly see that the physics of the problem was successfully simulated. And as illustration, we present in Fig. (12) the numerical solution at time $t = 10s$, when occurs the main vortical structure in the flow. Besides, in order to complement our presentation, we depicts in Fig. (13)-(a) the contours of pressure and the contours of the velocity field in (b) r and (c) z directions.

t = 0.25s

(a) **(b)**

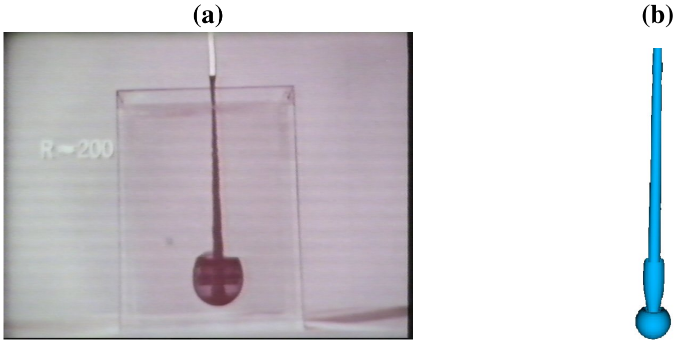

t = 0.75s

(a) **(b)**

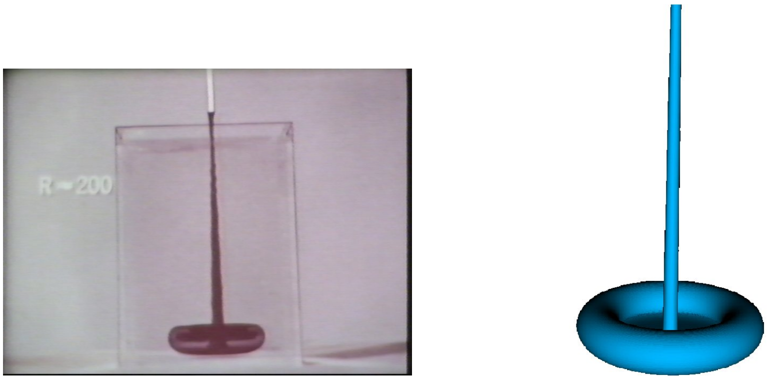

Figure 11. **Comparison of (a) experiments results and (b) numerical solution obtained by SDPUS-C1 scheme in the fluid vertical jet problem for** $Re = 200$ **in times** $t = 0.25s$ **and** $t = 0.75s$**.**

t = 10s

(a) **(b)**

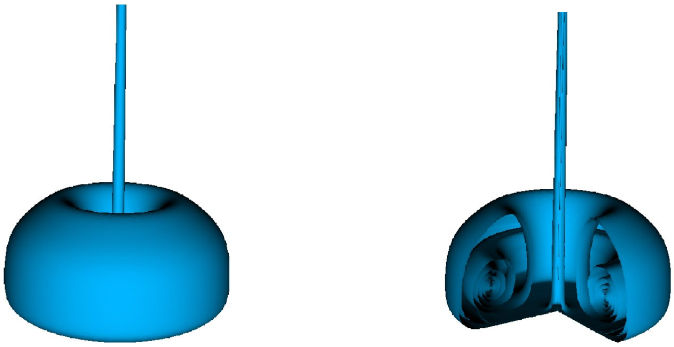

Figure 12. **Illustration of (a) complete structure and (b) structure with a cut in fluid vertical jet problem for** $Re = 200$ **and time** $t = 10s$**.**

5. CONCLUSION

We presented in this work a new polynomial upwind scheme, called SDPUS-C1, for numerical solution of conservation laws and related fluid dynamics problems. In particular, we simulated Riemann problems for the shallow water, acoustic and Euler equations. In these linear and nonlinear test cases, the SDPUS-C1 scheme showed good performance. Then, as application, we applied the SDPUS-C1 scheme for solving the dynamics of a vertical free jet penetrating into a recipient with the same fluid at rest, whose numerical results showed to be in accordance with the experimental results.

In summary, from the numerical results, the reader can infer that the upwinding SDPUS-C1 scheme is a robust tool to solve both complex compressible and incompressible flow problems. For future, the authors are planning to use this shock capturing upwind scheme for solving 3D incompressible fluid flows involving moving free surface.

6. ACKNOWLEDGMENTS

We gratefully acknowledge the support provided by FAPESP (Grants 2008/07367-9 and 2008/01258-3), CNPq (Grants 133446/2009-3, 300479/2008-5 and 573710/2008-2 (INCT-MACC)), CAPES (Grant PECPG1462/08-3) and FAPERJ (Grant E-26/170.030/2008 (INCT-MACC)).

7. REFERENCES

Castelo, A., Tomé, M.F., McKee, S., Cuminato, J.A. and Cesar, C.N.L., 2000, “Freeflow: an integrated simulation system for three-dimensional free surface flows”, *Journal of Computers and Visualization in Science*, Vol. 2, pp. 1-12.

Ferreira, V.G., Kurokawa, F.A., Queiroz, R.A.B., Kaibara, M.K., Oishi, C.M., Cuminato, J.A., Castelo, A., Tomé, M.F. and McKee, S., 2009, “Assessment of a high-order finite difference upwind scheme for the simulation of convection-diffusion problems”, *International Journal for Numerical Methods in Fluids*, Vol. 60, pp. 1-26.

Gaskell, P.H. and Lau, K.C., 1988, “Curvature-compensated convective transport: Smart, a new boundedness preserving transport algorithm”, *International Journal of Numerical Methods in fluids*, Vol. 8, pp. 617-641.

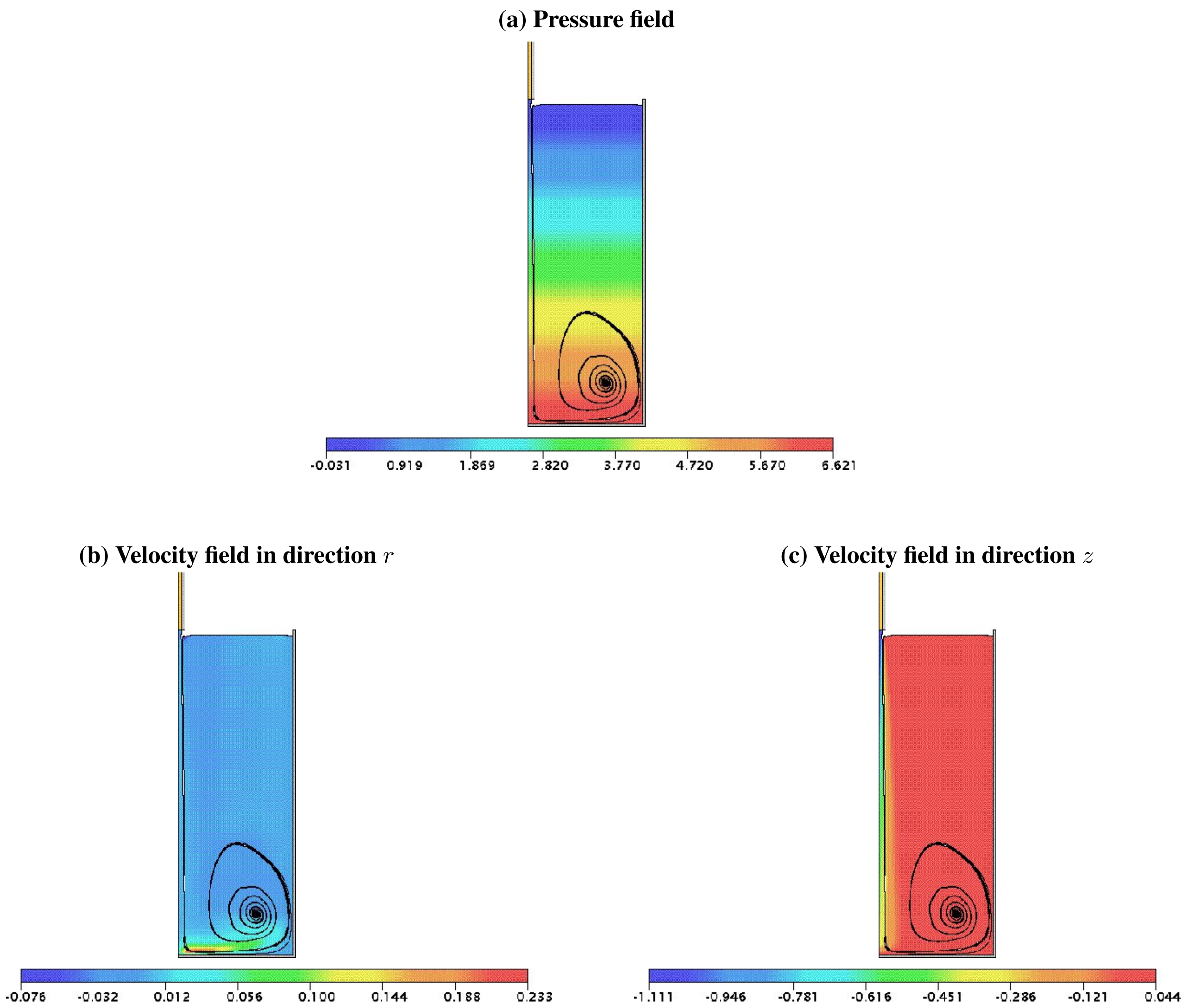

Figure 13. **Pressure and velocities fields obtained by SDPUS-C1 scheme at** $Re = 200$ **and time** $t = 10s$**.**

Harten, A., 1983, "High resolution schemes for hyperbolic conservation laws", *Journal of Computational Physics*, Vol. 49, pp. 357-393.

Leonard, B.P., 1988, "Simple high-accuracy resolution program for convective modeling of discontinuities", *International Journal for Numerical Methods in Fluids*, Vol. 8, pp. 1291-1318.

LeVeque, R.J., 2002, "Finite volumes methods for hyperbolic problems", *Press Syndicate of the University of Cambridge*.

Lin, H. and Chieng, C. C., 1991, "Characteristic-based flux limiters of an essentially third-order flux-splitting method for hyperbolic conservation laws", *International Journal for Numerical Methods in Fluids*, Vol. 13, pp. 287-307.

Ricchiuto, M., Csik, A., and Deconinck, H., 2005, "Residual distribution for general time-dependent conservation laws", *Journal of Computational Phisycs*, Vol. 209, pp. 249-289.

Taylor, G. I., 1974, "Low-reynolds number flows", National Commitee for Fluid Mechanics Films. *Illustrated experiments in fluid mechanics*.

Waterson, N. P. and Deconinck, H., 2007, "Design principles for bounded higher-order convection schemes - a unified approach", *Journal of Computational Physics*, Vol. 224, pp. 182-207.

Zijlema, M., 1996, "On the construction of a third-order accurate monotone convection scheme with application to turbulent flows in general domains", *International Journal for Numerical Methods in Fluids*, Vol. 22, pp. 619-641.

Yu, B., Tao, W.Q., Zhang, D.S. and Wang, Q.W., 2001,"Discussion on numerical stability and boundedness of convective discretized scheme", *Numerical Heat Transfer*, Vol. 40, pp. 343-365.

8. COPYRIGHT